

## Electronic Structure and Intrinsic Redox Properties of $[2\text{Fe}-2\text{S}]^+$ Clusters with Tri- and Tetracoordinate Iron Sites

You-Jun Fu,<sup>†‡</sup> Shuqiang Niu,<sup>§</sup> Toshiko Ichiye,<sup>§</sup> and Lai-Sheng Wang<sup>\*†‡</sup>

Department of Physics, Washington State University, 2710 University Drive, Richland, Washington 99352, W. R. Wiley Environmental Molecular Sciences Laboratory and Chemical Science Division, Pacific Northwest National Laboratory, P.O. Box 999, Richland, Washington 99352, and Department of Chemistry, Georgetown University, Washington, D.C. 20057-1227

Received October 15, 2004

Using potentially bidentate ligands ( $-\text{SC}_2\text{H}_4\text{NH}_2$ ), we produced  $[2\text{Fe}-2\text{S}]^+$  species of different coordination geometries by fission of  $[4\text{Fe}-4\text{S}]^{2+}$  complexes. Even though the ligands are monodentate in the cubane complexes, both mono- and bidentate complexes were observed in the  $[2\text{Fe}]$  fission products through self-assembly because of the high reactivity of the tricoordinate iron sites. The electronic structure of the  $[2\text{Fe}]$  species was probed using photoelectron spectroscopy and density functional calculations. It was found that tetracoordination significantly decreases the electron binding energies of the  $[2\text{Fe}]$  complexes, thus increasing the reducing capability of the  $[2\text{Fe}-2\text{S}]^+$  clusters.

The iron–molybdenum cofactor (FeMoco) is the site where nitrogenase reduces  $\text{N}_2$  to  $\text{NH}_3$ .<sup>1</sup> The originally determined structure<sup>2</sup> of FeMoco consisted of a  $\text{MoFe}_7\text{S}_9$  cluster in which six of the seven iron atoms in the cluster core exhibited the rare distorted trigonal geometry. The existence of an internal ligand atom X (X = C, N, or O) in the center of FeMoco was recently discovered.<sup>3</sup> This revision has been an incentive for chemists to synthesize structural models with the unusual three-coordinate, unsaturated iron sites.<sup>4</sup> However, these iron atoms are highly distorted in symmetry, and their interaction with the hypervalent ligand atom X is weak. Hence, the Fe–X bonds are most likely disrupted during catalysis, and the reactivity of the iron sites

are high.<sup>5</sup> Therefore, three-coordinate iron complexes, which have seldom been reported,<sup>6</sup> are still one of the best possible candidates being studied to mimic the reactive sites of FeMoco.<sup>7</sup> Here, we report a photoelectron spectroscopy (PES) study on a series of  $[2\text{Fe}-2\text{S}]$  clusters with various coordination geometries produced by collision-induced dissociation (CID) of  $[4\text{Fe}-4\text{S}]$  cubane complexes and the subsequent self-assembly in the gas phase.

A symmetric fission process of doubly charged  $[4\text{Fe}-4\text{S}]$  cubane anions into two identical singly charged  $[2\text{Fe}-2\text{S}]$  clusters with both iron sites tricoordinated was discovered previously in our group.<sup>8</sup> Considering the high reactivity of the three-coordinate iron site, we selected in the current work a potentially bidentate ligand, aminoethylethiol ( $-\text{SC}_2\text{H}_4\text{NH}_2$ ), to substitute the original monodentate ligand  $-\text{SEt}$  (Et =  $\text{C}_2\text{H}_5$ ) in  $[\text{Fe}_4\text{S}_4(\text{SEt})_4]^{2-}$  to form the precursor cubane complexes  $[\text{Fe}_4\text{S}_4(\text{SEt})_{4-n}\text{L}'_n]^{2-}$  ( $\text{L}' = -\text{SC}_2\text{H}_4\text{NH}_2$ ,  $n = 0-4$ ). We envisioned that self-assembly caused by the tricoordinate iron site might occur following the CID to generate  $[\text{Fe}_2\text{S}_2(\text{SEt})_{2-x}\text{L}'_x]^-$  ( $x = 0-2$ ) complexes with different geometries (Figure 1a).

\* To whom correspondence should be addressed. E-mail: ls.wang@pnl.gov.

<sup>†</sup> Washington State University.

<sup>‡</sup> Pacific Northwest National Laboratory.

<sup>§</sup> Georgetown University.

- (1) Burgess, B. K.; Lowe, D. J. *Chem. Rev.* **1996**, *96*, 2983. (b) Seefeldt, L. C.; Dance, I.; Dean, D. R. *Biochemistry* **2004**, *43*, 1401.
- (2) (a) Georgiadis, M. M.; Komiyama, H.; Chakrabarti, P.; Woo, D.; Kornuc, J. J.; Rees, D. C. *Science* **1992**, *257*, 1653. (b) Kim, J.; Rees, D. C. *Science* **1992**, *257*, 1677. (c) Kim, J.; Rees, D. C. *Nature* **1992**, *360*, 553. (d) Kim, J.; Woo, D.; Rees, D. C. *Biochemistry* **1993**, *32*, 7104.
- (3) Einsle, O.; Tezcan, F. A.; Andrade, S. L. A.; Schmid, B.; Yoshida, M.; Howard, J. B.; Rees, D. C. *Science* **2002**, *297*, 1696.
- (4) Lee, S. C.; Holm, R. H. *Proc. Natl. Acad. Sci.* **2003**, *100*, 3595.

- (5) (a) Lovell, T.; Liu, T.; Case, D. A.; Noodleman, L. *J. Am. Chem. Soc.* **2003**, *125*, 8377. (b) Kozak, C. M.; Mountford, P. *Angew. Chem., Int. Ed.* **2004**, *43*, 1186. (c) Hinemann, B.; Norskov, J. K. *J. Am. Chem. Soc.* **2004**, *126*, 3920. (d) Dance, I. *Chem. Commun.* **2003**, 324. (e) Schimpl, J.; Petrilli, H. M.; Blochl, P. E. *J. Am. Chem. Soc.* **2003**, *125*, 15772. (e) Huniar, U.; Ahlrichs, R.; Coucouvanis, D. *J. Am. Chem. Soc.* **2004**, *126*, 2588.
- (6) (a) MacDonnell, F. M.; Ruhlandt-Senge, K.; Ellison, J. J.; Holm, R. H.; Power, P. P. *Inorg. Chem.* **1995**, *34*, 1815. (b) Power, P. P.; Shoner, S. C. *Angew. Chem., Int. Ed. Engl.* **1991**, *30*, 330. (c) Sanakis, Y.; Power, P. P.; Stubna, A.; Munck, E. *Inorg. Chem.* **2002**, *41*, 2690. (d) Yang, X.; Wang, X. B.; Fu, Y. J.; Wang, L. S. *J. Phys. Chem. A* **2003**, *107*, 1703. (e) Yang, X.; Wang, X. B.; Wang, L. S.; Niu, S. Q.; Ichiye, T. *J. Chem. Phys.* **2003**, *119*, 8311. (f) Niu, S. Q.; Wang, X. B.; Nichols, J. A.; Wang, L. S.; Ichiye, T. *J. Phys. Chem. A* **2003**, *107*, 2898.
- (7) (a) Vela, J.; Stoian, S.; Flaschenriem, C. J.; Munck, E.; Holland, P. L. *J. Am. Chem. Soc.* **2004**, *126*, 4522. (b) Smith, J. M.; Lachicotte, R. J.; Pittard, K. A.; Cundari, T. R.; Lukat-Rodgers, G.; Rodgers, K. R.; Holland, P. L. *J. Am. Chem. Soc.* **2001**, *123*, 9222.
- (8) (a) Yang, X.; Wang, X. B.; Niu, S. Q.; Pickett, C. J.; Ichiye, T.; Wang, L. S. *Phys. Rev. Lett.* **2002**, *89*, 163401. (b) Yang, X.; Wang, X. B.; Wang, L. S. *Int. J. Mass Spectrom.* **2003**, *228*, 797.

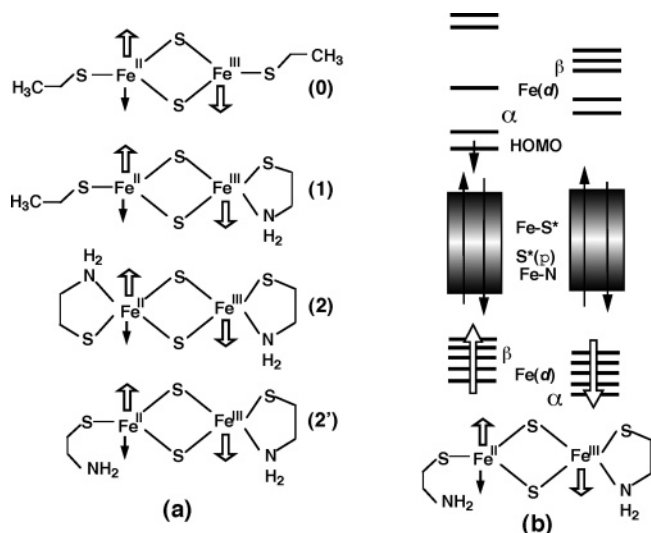


**Figure 1.** (a) Schematic structures of the [2Fe–2S] clusters with different coordination geometries. (b) Schematic molecular orbital energy diagram of 2' showing the difference between tri- and tetra-coordinate iron sites. The large arrows represent the d<sup>5</sup> majority-spin electrons on each Fe, and the small arrows represent the minority-spin electron.

The experiments were carried out using a PES apparatus equipped with an electrospray source and a magnetic-bottle TOF photoelectron analyzer.<sup>9,10</sup> CID experiments on [Fe<sub>4</sub>S<sub>4</sub>(SEt)<sub>4-n</sub>L'<sub>n</sub>]<sup>2-</sup> were carried out by applying a voltage of 2.5–6 V to the first skimmer of the instrument.<sup>8,9</sup> Complete CID of the [4Fe–4S] cubanes could be obtained when the mass peaks of the two species with  $n = 1$  and 3 disappeared from the mass spectrum (Figure S1).<sup>11</sup> In the PES experiment, two detachment photon energies were used: 266 nm (4.661 eV) from a Nd:YAG laser and 193 nm (6.424 eV) from an ArF excimer laser.

The PES spectra at the two photon energies for the ligand-substituted [Fe<sub>4</sub>S<sub>4</sub>(SEt)<sub>4-n</sub>L'<sub>n</sub>]<sup>2-</sup> complexes (Figure 2) are very similar to that of [Fe<sub>4</sub>S<sub>4</sub>(SEt)<sub>4</sub>]<sup>2-</sup>.<sup>10</sup> Significant spectral cutoffs were observed in the higher-binding-energy side in each spectrum, typical of PES spectra for multiply charged anions due to the repulsive Coulomb barrier (RCB).<sup>12</sup> The adiabatic binding energy (ADE) increases sequentially from 0.29 to 0.66 eV with ligand substitution number  $n$  from 0 to 4 (Table S1).

The key results of this study are shown in Figure 3. The apparent difference in the PES spectra between [Fe<sub>2</sub>S<sub>2</sub>(SEt)<sub>2-x</sub>L'<sub>x</sub>]<sup>-</sup> and their [4Fe–4S] cubane parents is the significant increase in binding energy and the lack of spectral cutoffs, because of the absence of intramolecular Coulomb repulsion and RCB in the singly charged [2Fe–2S] products.<sup>12</sup> The species for  $x = 0$  and 1 showed spectral patterns similar to those of their corresponding [4Fe–4S] parents, exhibiting two features in the low electron binding energy

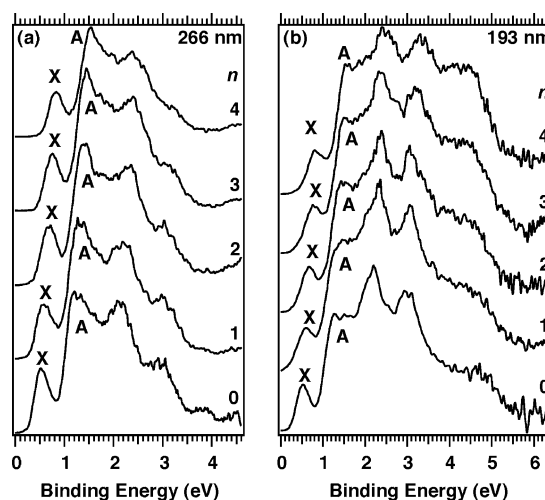


**Figure 2.** Photoelectron spectra of [Fe<sub>4</sub>S<sub>4</sub>(SEt)<sub>4-n</sub>L'<sub>n</sub>]<sup>2-</sup> ( $n = 0-4$ ) at (a) 266 and (b) 193 nm.

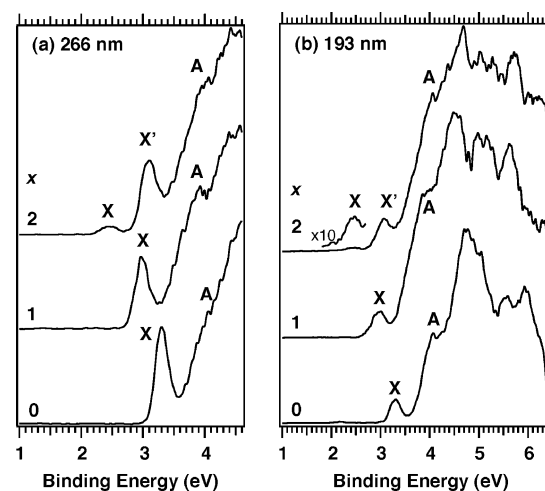


**Figure 3.** Photoelectron spectra of [Fe<sub>2</sub>S<sub>2</sub>(SEt)<sub>2-x</sub>L'<sub>x</sub>]<sup>-</sup> ( $x = 0-2$ ) at (a) 266 and (b) 193 nm.

range (X, A).<sup>8a</sup> However, in contrast to the binding energy increase for the [4Fe–4S] clusters as a function of L' substitution (Figure 2), a dramatic decrease in the electron binding energy was observed for [Fe<sub>2</sub>S<sub>2</sub>(SEt)<sub>2-x</sub>L'<sub>x</sub>]<sup>-</sup> from 3.14 eV at  $x = 0$  to 2.79 eV at  $x = 1$ . More surprisingly, an additional feature was observed in the spectra of [Fe<sub>2</sub>S<sub>2</sub>L'<sub>2</sub>]<sup>-</sup> (X' in Figure 3). The ADE measured from the threshold peak (X) is 2.24 eV, a 0.55-eV decrease from that of **1**. The second peak (X') at 3.10 eV (VDE) is much stronger, and its relative intensity is very similar to the threshold feature of species **1**.

Broken-symmetry DFT calculations, specifically with Becke's three-parameter hybrid exchange function and the Lee–Yang–Parr correlation function (B3LYP) using the 6-31G\*\* basis set,<sup>14,15</sup> were carried out for geometry optimizations and electronic structures of [Fe<sub>4</sub>S<sub>4</sub>L'<sub>4</sub>]<sup>2-</sup> and

(9) Wang, L. S.; Ding, C. F.; Wang, X. B.; Barlow, S. E. *Rev. Sci. Instrum.* **1999**, *70*, 1957.

(10) Wang, X. B.; Niu, S. Q.; Yang, X.; Ibrahim, S. K.; Pickett, C. J.; Ichiye, T.; Wang, L. S. *J. Am. Chem. Soc.* **2003**, *125*, 14072.

(11) The symmetric fissions of all five [Fe<sub>4</sub>S<sub>4</sub>(SEt)<sub>4-n</sub>L'<sub>n</sub>]<sup>2-</sup> ( $n = 0-4$ ) species can yield only three [2Fe–2S] products: [Fe<sub>2</sub>S<sub>2</sub>(SEt)<sub>2</sub>]<sup>-</sup>, [Fe<sub>2</sub>S<sub>2</sub>(SEt)L']<sup>-</sup>, and [Fe<sub>2</sub>S<sub>2</sub>L'<sub>2</sub>]<sup>-</sup>.

(12) (a) Wang, X. B.; Ding, C. F.; Wang, L. S. *Phys. Rev. Lett.* **1998**, *81*, 3351. (b) Wang, X. B.; Wang, L. S. *Nature* **1999**, *400*, 245.

(13) (a) Li, J.; Nelson, M. R.; Peng, C. Y.; Bashford, D.; Noodleman, L. *J. Phys. Chem. A* **1998**, *102*, 6311. (b) Noodleman, L.; Baerends, E. J. *J. Am. Chem. Soc.* **1984**, *106*, 2316. (c) Norman, J. G., Jr.; Ryan, P. B.; Noodleman, L. *J. Am. Chem. Soc.* **1980**, *102*, 4279. (d) Noodleman, L.; Norman, J. G. Jr.; Osborne, J. H.; Aizman, A.; Case, D. A. *J. Am. Chem. Soc.* **1985**, *107*, 3418.

(14) Parr, R. G.; Yang, W. *Density-Functional Theory of Atoms and Molecules*; Oxford University Press: Oxford, U.K., 1989.

$[\text{Fe}_2\text{S}_2\text{L}'_2]^-$ .<sup>16</sup> The calculated oxidation energies were refined at B3LYP/6-31(++)G\*\*, where sp-type diffuse functions were added to the 6-31G\*\* basis set of the sulfur atoms.<sup>6,10</sup> For the cubane complex,  $\text{L}'$  prefers to be monodentate in a folded cis conformation, directing the dipole of the amino group toward the cubane core. The calculated ADE and VDE were 0.63 and 0.98 eV, respectively, in very good agreement with the experimental values of 0.66 and 0.83 eV. On the other hand, our DFT calculations showed that, if the  $\text{L}'$  ligands are bidentate in the cubane complex, the structure is less stable by 23.5 kcal/mol and gives a very low electron binding energy ( $<0$ ). Thus, we conclude that  $\text{L}'$  in  $[\text{Fe}_4\text{S}_4(\text{SEt})_{4-n}\text{L}'_n]^{2-}$  acts as a monodentate ligand and that it is the electrostatic interaction between the polar amino group and the cubane core that causes the electron binding energy to increase for the substituted cubane species (Figure 2), similarly to other mixed-ligand cubanes.<sup>17</sup>

On the other hand, our DFT results on  $[\text{Fe}_2\text{S}_2\text{L}'_2]^-$  showed that  $\text{L}'$  favors a bidentate coordination in the  $[\text{2Fe}-\text{2S}]$  cluster in contrast to that in the  $[\text{4Fe}-\text{4S}]$  complex. In particular, we found that  $\mathbf{2}'$  with one tetracoordinated  $\text{Fe}^{\text{III}}$  is more stable by 14.8 kcal/mol than the structure in which both iron sites are tricoordinated such as that in  $\mathbf{0}$  (Figure 1). However, if the  $\text{Fe}^{\text{II}}$ , instead of the  $\text{Fe}^{\text{III}}$ , site in  $\mathbf{2}'$  is tetracoordinated, the stabilization is only 5.5 kcal/mol relative to the structure with two tricoordinated Fe. This result is consistent with our recent study on the mononuclear complexes showing that  $\text{Fe}^{\text{II}}$  prefers tricoordination whereas  $\text{Fe}^{\text{III}}$  prefers tetracoordination.<sup>6f</sup> In the current study, we found that isomer  $\mathbf{2}$  is more stable than  $\mathbf{2}'$  by only 1.2 kcal/mol.

A schematic molecular orbital energy diagram of isomer  $\mathbf{2}'$  is shown in Figure 1b.<sup>6f,13</sup> The HOMO of  $[\text{Fe}_2\text{S}_2(\text{SEt})_{2-x}\text{L}'_x]^-$  is a singly occupied ferrous  $d_{z^2}$  orbital, which arises from the interaction with the lone pair of the ligand and has  $\sigma_{\text{Fe}-\text{L}'}$  antibonding character. Thus, chelating interactions of  $\text{L}'$  with the ferrous center would push the HOMO upward and significantly decrease its electron binding energy by  $\sim 0.8$  eV. On the other hand, the bidentate coordination of  $\text{L}'$  to the ferric center increases both the  $\text{Fe}^{\text{III}}-\text{S}$  bond lengths and the charges on the bridging sulfide, resulting in the lower-lying sulfide lone pair and decreasing the bonding interactions between the bridging sulfides and the ferrous center. Thus, it indirectly leads to the increase of the bonding interaction between  $\text{L}'$  and the ferrous center, pushing the HOMO upward and decreasing the electron binding energy by  $\sim 0.5$  eV.

(15) Hehre, W. J.; Radom, L.; Schleyer, P. V. R.; Pople, J. A. *Ab initio Molecular Orbital Theory*; John Wiley & Sons: New York, 1986.

(16) All DFT calculations were performed using NWChem, A Computational Chemistry Package for Parallel Computers, version 4.5.; Pacific Northwest National Laboratory: Richland, WA, 2003.

(17) Fu, Y. J.; Yang, X.; Wang, X. B.; Wang, L. S. *Inorg. Chem.* **2004**, *43*, 3647.

The DFT results are in good agreement with the experimental observation (Figure 3). The decrease of electron binding energies in  $\mathbf{1}$  relative to  $\mathbf{0}$  is a strong indication of the bidentate coordination of  $\text{L}'$  to the ferric center. The observed decrease of 0.35 eV (Table S1) is consistent with the DFT result of  $\sim 0.5$  eV. If  $\text{L}'$  in  $\mathbf{1}$  were monodentate, we would expect an increase of electron binding energies due to the electrostatic interactions of the polar  $-\text{NH}_2$  group, as observed for the cubane complexes (Figure 2).<sup>17</sup> For  $[\text{Fe}_2\text{S}_2\text{L}'_2]^-$ , two isomers ( $\mathbf{2}$  and  $\mathbf{2}'$ ) are possible.  $\mathbf{2}$  would result in a further decrease of the electron binding energies relative to  $\mathbf{1}$  because of the tetracoordinated ferrous center, whereas  $\mathbf{2}'$  would result in an increase in electron binding energy relative to  $\mathbf{1}$  because of the electrostatic interaction of the uncoordinated  $-\text{NH}_2$  group. In fact, both  $\mathbf{2}$  and  $\mathbf{2}'$  were observed in the PES experiment (Figure 3). The weak feature X is readily assigned to  $\mathbf{2}$ : its binding energy is lower than that of  $\mathbf{0}$  by 0.9 eV, in very good agreement with the DFT value of 0.8 eV. The stronger feature X' is assigned to  $\mathbf{2}'$ : its electron binding energy is increased by 0.23 eV relative to that of  $\mathbf{1}$ , consistent with the expected electrostatic effect of the  $-\text{NH}_2$  group. We note that the 0.64-eV difference in the electron binding energies between  $\mathbf{2}$  and  $\mathbf{2}'$  represents a pure structural effects on the electron binding energy of the  $[\text{2Fe}-\text{2S}]$  center. The intensity ratio for the peaks X and X' ( $\sim 0.11$ ) suggested that, in our experiment,  $\sim 10\%$  of the fission product was isomer  $\mathbf{2}$  and  $\sim 90\%$  was isomer  $\mathbf{2}'$ . Our DFT results suggested that  $\mathbf{2}$  is slightly more stable than  $\mathbf{2}'$  by  $\sim 1.2$  kcal/mol. This observation apparently indicated that the formation of  $\mathbf{2}$  and  $\mathbf{2}'$  was kinetically controlled.

In summary, both PES experiments and DFT calculations suggest that the bidentate coordination of the  $[\text{2Fe}-\text{2S}]$  cluster results in significantly lower electron binding energies, thus increasing its reducing power as a redox center. This observation might be relevant to understanding the electronic structure of FeMoco and might suggest further insight into the role of the central atom X.

**Acknowledgment.** This work was funded by the National Institutes of Health (GM-63555 to L.S.W. and GM-45303 to T.I.). The experimental work was performed at the EMSL, a national user facility sponsored by the U.S. DOE's Office of Biological and Environmental Research and located at Pacific Northwest National Laboratory, operated for the DOE by Battelle.

**Supporting Information Available:** Electrospray mass spectra, table of electron binding energies. These materials are available free of charge via the Internet at <http://pubs.acs.org>.

IC048559D